SOILS2SEA DELIVERABLE NO. 4.2

BONUS
SCIENCE FOR A BETTER FUTURE OF THE BALTIC SEA REGION

Tracer tests and the effect of solute retention and attenuation on the stream reach scale

SOILS2SEA

Reducing nutrient loadings from agricultural soils to the Baltic Sea via groundwater and streams

This page has intentionally been left blank

SOILS2SEA DELIVERABLE NO. 4.2

Tracer Tests and the effect of solute retention and attenuation on the stream reach scale

December 2016

Authors:
Joakim Riml, The Royal Institute of Technology
Ida Morén, The Royal Institute of Technology
Anders Wörman, The Royal Institute of Technology
Damian Zięba, AGH University of Science and Technology
Przemyslaw Wachniew, AGH University of Science and Technology

SOILS2SEA

Reducing nutrient loadings from agricultural soils to the Baltic Sea via groundwater and streams

This report is a publicly accessible deliverable of the Soils2Sea project. The present work has been carried out within the project 'Reducing nutrient loadings from agricultural soils to the Baltic Sea via groundwater and streams (BONUS Soils2Sea)', which has received funding from BONUS, the joint Baltic Sea research and development programme (Art 185), funded jointly from the European Union's Seventh Programme for research, technological development and demonstration and from Innovation Fund Denmark, The Swedish Environmental Protection Agency (Naturvådsverket), The Polish National Centre for Research and Development, The German Ministry for Education and Research (Bundesministerium für Bildung und Forschung), and The Russian Foundation for Basic Researches (RFBR).

This report may be downloaded from the internet and copied, provided that it is not changed and that it is properly referenced. It may be cited as:

J Riml, I Morén, A Wörman, D Zięba, and Przemyslaw Wachniew. Tracer Tests and the effect of solute retention and attenuation on the stream reach scale. BONUS Soils2Sea Deliverable 4.2. Royal Institute of Technology (KTH), Stockholm, December 2016, www.Soils2Sea.eu

Table of Contents

1. Summary

This report describes the first major stream-tracer test using $^{3}H_2O$, $^{32}PO_4^-$ (in the form of phosphate acid), $^{15}NO_3^-$ (in the form of potassium nitrate) and tritium labeled water. A main reason for using tririated water ($^{3}H_2O$) is that this gives an independent signal of the hydrological response of the stream system that can be used to interpret the transport of reactive solutes represented by the signals of $^{32}PO_4^-$ and $^{15}NO_3^-$. A main purpose of the report is

a) To use the tracer approach for quantification of the effect of remediation actions in agricultural streams
b) To describes the tracer injection methodology, safety aspects and evaluation methods.

The report also describes several independently conducted tracer tests using Rhodamine WT in the same stream. All solutes were simultaneously injected in Tullstorps Brook, Skåne, Sweden, using a pump system and concentration vs. time (so-called breakthrough) curves were determined from water samples taken at five (5) downstream located sampling stations. This report describes the tracer injection methodology, safety aspects of radioactive tracer injections, basic evaluation methods for breakthrough curves and tentative results in the form of certain model parameters. Prior to the main tracer test an extensive field campaign was conducted in Tullstorps Brook with the objective to gain general knowledge about the hydrodynamic behavior of the system, including Rhodamine WT tracer tests and independent measurements of the stream hydro-morphology. Methodologies and results from this field campaign are also included in the report.

2. Introduction

Surface water offer important transport conduits for contaminants from the land to the oceans, especially diffuse contaminants like nutrients applied in agriculture. About half of the nitrogen and phosphorus supplied to the Baltic Sea are transported there through streams and rivers, although the trend is slightly decreasing in recent decades (Monitior, 1988; Fölster et al., 2012). The transport dynamics of flowing surface waters is therefore a crucial part of the eutrophication of aquatic environments and the ecological effects of recipient waters. An important aspect is the natural degradation and retention of both phosphorus and nitrogen in certain stream environments, herein referred to as self-cleaning, which can be included in the planning of the land management of the river basin (Andersson and Arheimer, 2003; Arheimer et al., 2005). A key process in such self-cleaning is the filtering of water and chemical reactions that occurs in the hyporheic or lateral zones of the stream due to meandering and hydraulic head induced vertical exchange (Elliott and Brooks, 1997; Wroblicky, 1998; Wörman et al., 2002; Boano et al., 2014). Several biogeochemical mechanisms occurring in the lateral and hyporheic zones, such as adsorption on available solid surfaces and denitrification in biofilms, can enhance retention and reduction of nutrients.

Despite extensive knowledge of uptake mechanisms and hyporheic reactions (Boano et al., 2015; Cardenas, 2015) a fully simultaneous stream tracer test with phosphate, nitrate and an inert solute representing the fate of water has never been conducted. Monitoring data can be very useful for the calibration of interpretative models and for the understanding of long-term variability in transport behavior. However, existing monitoring programs are commonly quite sparse in time, which may prohibit a detailed interpretation of basic hydrological and biogeochemical mechanisms, to the extent that the behavior of various solute substances is difficult to distinguish. The aim of this study was to perform the first major stream-tracer test using $^{32}PO_4^-$ (in the form of phosphate acid), $^{15}NO_3^-$ (in the form of potassium nitrate) and tritium labeled water. All solutes were simultaneously injected in Tullstorps Brook, Skåne, Sweden, using a pump system and concentration vs. time (so called breakthrough) curves were determined from water samples taken at five (5) downstream located sampling stations. This report describes the tracer injection methodology, safety aspects of radioactive tracer injections, basic evaluation methods for breakthrough curves and tentative results in the form of certain model parameters. Prior to the main tracer test an extensive field campaign was conducted in Tullstorps Brook with the objective to gain general knowledge about the hydrodynamic behavior of the system, including Rhodamine WT tracer tests and independent measurements of the stream hydro-morphology. Methodologies and results from this field campaign are also included in the report.

3. Methods

3.1 General description of Tullstorps Brook

The Tullstorps Brook is a small agricultural stream located in Trelleborgs Municipality, Region of Skåne, Sweden which is discharging into the Baltic Sea at the most southern point of Sweden in the village of Smygehuk (Figure 1 and Figure 5). The stream has a catchment area of around 63 km^2 and an estimated yearly average discharge of around 0.5 m^3/s (Olofsson, 2015). 85 % of the catchment consists of agricultural land. Due to extensive farming, high nutrient levels have been observed at the outlet of the stream and the Water Framework Directive did classify the stream as in "Bad Ecological Chemical Status" in 2006 as well as 2012. During the period of 2001-2006 the yearly average total phosphor concentration (TP) and total nitrogen concentration (TN) was measured to be 134 µg/L respective 7.53 mg/L, and although nutrient levels decreased slightly to TP = 139 µg/L and TN = 4.84 mg/L between 2006 and 2012 the concentrations were still far above the level for good status (VISS, 2016). To improve the ecological status of the stream an economical association among farmers within the catchment was started with support from the Environmental Department and regional county 2008, with the aim to keep nutrients at the fields, prevent eutrophication of the recipient (The Baltic Sea) and to manage problems with flooding (Svensson, 2014). Since then, the stream has been the object of an extensive restoration campaign including remeandering, widening of the riparian zone, alteration of vegetation types and patterns and construction of sediment traps and wetlands in connection to the main stream channel. Also logs, boulders and new sediments have been placed at the stream bottoms. Continuous measurements at the outlet of the stream indicates that the TP concentration has decreased 10-20% since the project started, which is a larger change than what has been observed in other streams in the area during the same time period, while no general decreasing trend in the TN concentrations has been observed (Olofsson, 2015). In total, 6 km of the total 20 km long stream has been modified from a channelized ditch (pre-remediation) to resemble more pristine conditions (post-remediation).

The objectives of the remediation actions are to slow down the transportation of water and solutes and to increase the connectivity between the main stream channel and biogeochemically active hyporheic and lateral zones. With the intention to closely study the self-cleaning capacity of streams in general and the importance of transient storage zones specifically, tracer tests were performed in the Tullstorps Brook at several occasions, both in the post-restored and pre-restored parts of the stream, covering a total stream length of 5,700 m. To understand the hydrodynamic as well as the biogeochemical processes controlling the retention of nutrients in streams conservative and reactive tracers were used separately and together. An introductory field campaign including several tracer tests with the fluorescent tracer Rhodamine WT (RWT)

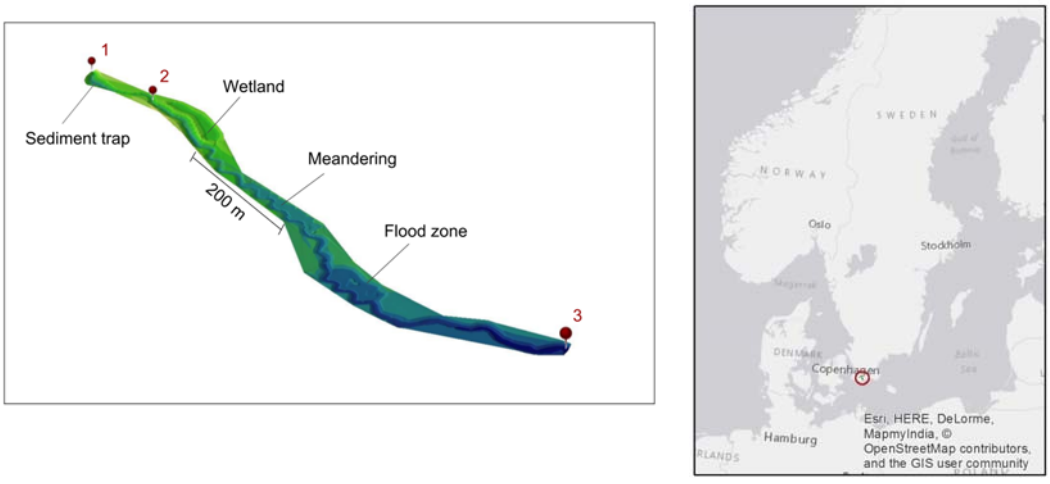

Figure 1. (a) Examples of remediation measures in the Tullstorps brook reach R1-2 and R2-3 (see extension of reaches in figure 5). (b) Location of the Tullstorps brook catchment.

and independent measurements of the stream geomorphology were performed during the summers of 2014 and 2015. Later, in December 2015, the main tracer tests with tritiated water, phosphorous and nitrogen isotopes were performed in the Tullstorps Brook.

3.2 Independent measurements of stream hydro-morphology

In order to get a general understanding of the hydrodynamic processes controlling retention of solutes in streams, independent measurements of hydro-morphological parameter can be central to assist tracer test evaluation and predict general trends in retention. Measuring stream characteristics such as average stream velocity, bed slope, hydraulic conductivity and dimensions of major geomorphological features at the stream bed can improve predictions of hydrodynamic retention with orders of magnitude (Boano et. al., 2014). In this study stream width and stream depth was measured in conjunction with all tracer tests using a measuring tape. The density of measures varied between every 100 m and 2 measures per stream reach and average parameters for the investigated reaches are summarized in Table 2 and 6. Lengths and slopes of different parts of the stream were evaluated from maps made by the Swedish Geological Survey. Furthermore, hydraulic conductivity of the stream bed sediments were measured every 100 meter along 5700 m of the Tullstorps brook (Figure 2). The measurements were done at two depths using a piezometer that was placed into the stream sediment and filled with water. The infiltration time of the water was then measured, by noting the decrease of water level in the piezometer with time, and related to the hydraulic conductivity. The estimated hydraulic conductivity was found to be relatively constant along the stream and had a total average of K = 8.5 10^{-3} m/s. At the downstream part of the study reach, the hydraulic conductivity was found to be decreasing and at the same time displaying a smaller spatial variability. This trend is probably caused by increased sedimentation of organic particles due to lower stream gradients and lower flow velocities as the stream approaches its effluence to the Baltic Sea.

Hydraulic head variations along the stream bottom can force surface water to enter into the stream-bed sediments and lateral zones were hydrodynamic and biogeochemical reactions are more prone to occur (e.g. Boano et al., 2014). In connection with one of the tracer tests, in August 2015, measurements of the hydraulic head variations were therefore done along a 455 m long stretch of the stream (Figure 3). The hydraulic head H_s (m) at the stream bottom can be divided into a static part, consisting of the potential energy of the stream-bed elevation z (m) and the stream water depth d(m), i.e. $H_s = z + d$, and a hydrodynamic part H_d, due to a fraction φ of the velocity head $u^2/(2\,g)$ (m) transferred into stagnation pressure when water is flowing over the rough surfaces, where u = mean flow velocity (m/s) and g = acceleration due to gravity (m/s^2), i.e. $\varphi\, u^2/(2\,g)$. Measurements of water and bed surface elevations were done using a leveling instrument every 4-7 m. At each cross-section the area (A [m^2]) perpendicular to the streamflow direction were observed using a measuring tape. The hydraulic mean depth of the stream d = A/w [m], where w is the stream width [m] at the water surface and A = the cross section area.

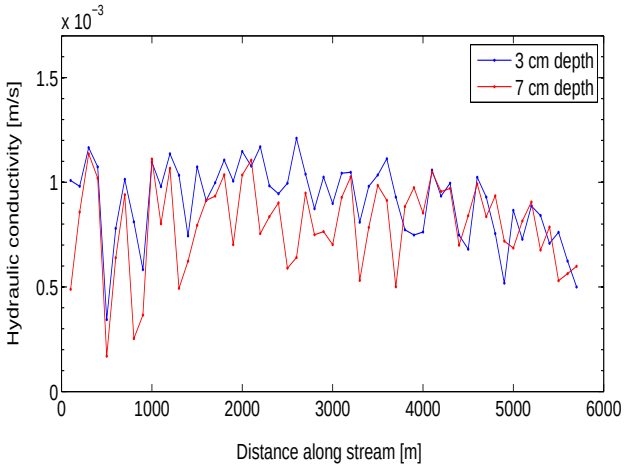

Figure 2. Hydraulic conductivity measurements along the Tullstorps brook at 3 and 7 cm depth.

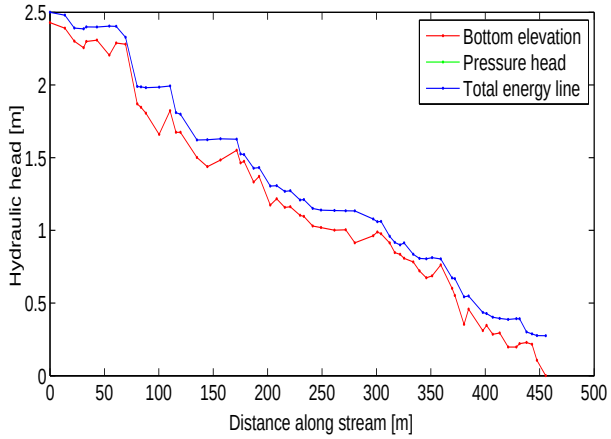

Figure 3. Hydraulic head measurements, presented as the bottom elevation only and the full pressure head, along a 455 m long stream reach from sampling point 5 and downstream (map in Figure 4). The velocity head is too small in comparison with the pressure head for the two to be plotted together in this scale, explaining why there is no visual difference between the pressure head and the total energy line.

The cross sectional area was used to calculate variances in the stream velocity that were related directly to the hydrodynamic head variations.

The resulting total hydraulic head (energy line) decreases along the stream reach and varies as a result of variations in the stream bottom profile (Figure 3). Variations in hydraulic conductivity and hydraulic head along the streambed are factors that drive hyporheic exchange and the measures can be used to validate scaling functions that link hydro-morphological parameters to hyporheic exchange and nutrient retention. This aspect is outside the scope of this report but will be reflected upon in future scientific papers.

3.3 Rhodamine WT tracer testing

RWT is a fluorescent tracer which over the years has been used in numerous hydrologic studies in both surface and groundwater (eg. Kunkel and Radke, 2011; Wilson et al., 1986). Although often used as a conservative tracer, some studies have shown that RWT is subjected to geochemical reactions, specifically adsorption onto organic materials in storage zones (Runkel, 2015). Nevertheless it was used in this study to learn more about the hydrodynamic response of the stream prior to the reactive tracer test, since it is an inexpensive tracer and it facilitates situ measurements for its simplicity. Further, the evaluation methods available do include ways to account for possible adsorption and, hence, to separate the hydrological processes affecting both inert and less inert solutes (chapter 2.5)

3.3.1 Risk assessment of RWT tracer test

Before the tracer test a risk analysis was carried out containing a literature study and simulation of tracer transportation in the Tullstorps Brook. Several studies have been performed regarding the toxicity of Rhodamine WT and the majority of studies have shown little impact on humans and aquatic organisms. According to Field et al. (1995) there is no risk for health effects on humans as long as the concentration of Rhodamine WT in drinking water does not exceed 2 mg/l, giving the concentrations are decreasing to normal levels within 24 hours. The study assumes that an adult human (70 kg) consumes 2 liters of water orally during a day and that the lethal dose of a rat can be assumed to be the same as for a human. Rowinski and Chirzanowski (2011) examined and compared the effect of Rhodamine WT and Rhodamine B on small aquatic organisms using so-called bio-indication. They discovered that some species shows a direct reaction to low concentrations of Rhodamine WT (0.1 mg/l), but the reactions of escape caused by increased concentrations quickly decrease when organisms become adapted to their new environment. According to the survey the dose of Rhodamine WT fatal for crustacean

Table 1 Deathly doses, $LC50_{96h}$ and $LC50_{48h}$ for three different organisms (modified form Field et al., 1995)

Substance	$LC50_{96h}$, Fish	$LC50_{48h}$, Cladocera	$LC50_{96h}$, Algae
Rhodamine WT	320 mg/l	170 mg/l	20 mg/l

Thamnocephalus platyurus is 1698 mg/L in 24 hours. Table 1 shows the lethal doses (LC50) defined in another study, for three aquatic animals after 96 hours and 48 hours respectively (Field et al., 1995).

Depending on the current flow rate different amounts of tracer is needed to perform a reliable evaluation of the breakthrough curves of tracer concentrations along the full investigated stream reach. When planning the tracer tests in Tullstorps Brook a concentration at the injection site of maximum 1 mg/l (calculations according to Wilson et al., 1986) was aimed for. The concentration are then rapidly diluted, resulting in concentrations below 0.01 mg/l within 2000 m (about 6 hours based on mathematical modeling of the transport of Rhodamine WT in Tullstorps Brook (see transport equations in chapter 2.5). Since the proposed concentration is below the concentrations shown to have an impact on humans or the environment and the experiment was expected to last for a limited amount of time, the risk for humans and the environment induced by the tracer test is conceived to be negligible. The risk for people in the area decreases further since Tullstorpsån is neither used for bathing nor for drinking.

3.3.2 In situ measurements of RWT concentration

When fluorescent substances are radiated with light, the energy is adsorbed and the molecule transformed into an exited state. The energy is then emitted in the form of light with lower frequencies and longer wavelength than the adsorbed light, which is a signal that can be measured with specific sensing devises (Wilson et. al., 1986). During the tracer test, the RWT florescence was measured in situ, using Cyclopes 7 fluorimeters (Turner Designs, Sunnyvale, CA). The fluorimeter, which was positioned in the stream, radiates light trough a LED lamp and measures the resulting emissions form RWT. Although measurements are done continuously, registration of the power of the signal was done every 30 sec in mV. To relate the power of the signal to concentration RWT a calibration curve is needed. In this study it was created by mixing known masses of RWT with stream water from the site and fitting a linear concentration-voltage curve to the data. The calibration curve applied in one of the experiments is seen in Figure 4.

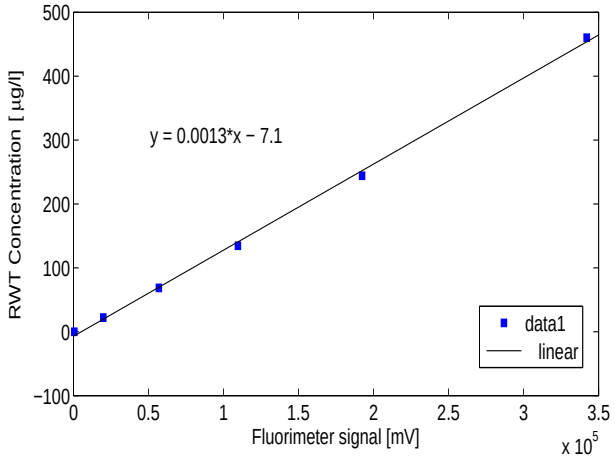

Figure 4. Example of RWT calibration curve transforming signals form mV to concentrations RWT (µg/l). Blue dots indicate RWT concentrations and fluorimeter signals prepared and measured in the lab. Concentrations were prepared using water from sampling site 4 taken in connection with the tracer test at 10th of June 2015. The equation of the linear fit is shown in the figure. $R^2 = 0.99$.

3.3.3 Performance of the RWT tracer injection and the evaluated stretches

Four tracer tests were performed in the Tullstorps Brook during the years 2014-2015. The tracer was injected as slug injections, at four different sites on four different occasions (Table 2). The injection mass was prepared at the injection site, using a scale, and injected by manually pouring the tracer into the stream and rinsing the bucket thoroughly. When choosing an injection site it is important to have fast flowing water, preferably supercritical conditions and high turbulence, in order for the tracer to spread out and mix across the channel before the first tracer sampling site (Kilpatrick and Wilson, 1989).This is because it is often assumed that complete mixing within the cross-sections prevails, both regarding sampling strategies and for model formulations of the tracer transportation (see section 2.5). Injections were made in the evening to avoid photodegradation of RWT and disturbance effects from sunlight on the fluorescence measuring devises.

The in-situ measurements were performed with the objective to be able compare the hydrodynamic response before and after remediation actions performed on reaches of special geomorphological and hydrodynamic characteristics. The reaches investigated with RWT are marked with pink on the map (Figure 5) and indexed with an R (for Rhodamine WT) together with the two sampling point surrounding the reach (eg, R1-2). All together two reaches that was remediated in 2009 and mapped in Figure 1a (R1-2 and R2-3), two channelized reaches (R4-5 and R6-7) and one reach of a more pristine character (R5-6) were investigated using RWT. The remediated reaches differ in the way that the upstream one consists of a single sediment trap while the downstream one consists of a variety of measures, including structures retaining surface water in flooding zones and 2-step ditches (the implemented measures are illustrated graphically in figure 1a). However, at the time of the tracer tests, the discharge was low leading to low water levels and no water flow through the subside flooding zones and 2-step-ditches. The characteristics of the five different reaches and the dates for the tracer tests performed in those reaches are summarized in Table 2.

Table 2 Dates of the performed tracer test and characteristics of the investigated reaches at the discharge conditions

		Reach characteristics		
Reach No: Date	Reach type	X (m)	d (m)	w (m)
R1-2: 27/08-2014	**Established remediation actions (Sediment trap):** A deepening and widening of the stream channel aiming to slow down the water and allowing particles to sediment. Densely vegetated.	80	1.5	6
R2-3: 27/08-2014	**Established remediation actions:** A variety of measures including engineered meandering, constructed riffle and pools. Objects such as boulders and logs evenly placed out along the stream bottom. Densely vegetated.	520	0.28	2.45
R4-5: 10/06-2015	**Non-remediated agricultural:** Channelized stream with steep and relatively small riparian zone. Few objects were present at the stream bottom.	1530	0.25	1.85
R5-6: 08/06-2015	**Non-remediated natural:** Slightly meandering reach with riffle and pool structure formed by natural boulders. Little vegetation in stream.	480	0.11	2.59
R6-7: 29/08-2015	**Non-remediated agricultural:** Channelized stream with steep and relatively small riparian zone. Few objects were present at the stream bottom.	1429	0.24	2.14

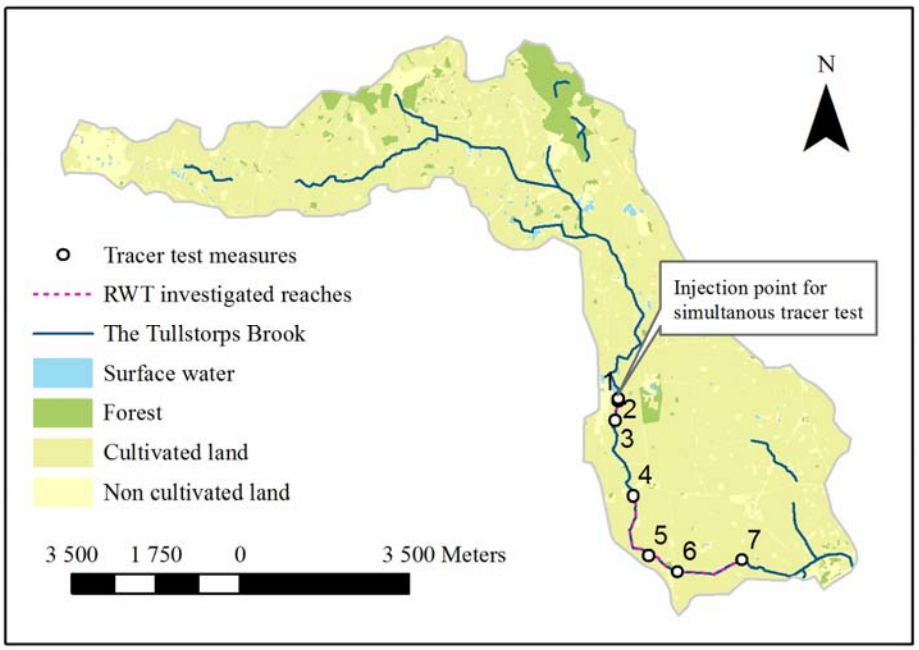

Figure 5. Map of the Tullstorps brook catchment area with general tracer test measuring points (1-7) and the injection point for the simultaneous tracer test using $^{3}H_2O$, $^{32}PO_4$ and $^{15}NO_3^-$. The injection points for the RWT tracer tests are not marked on the map but the reaches investigated with RWT is indicated with pink colour.

3.4 Simultaneous stream tracer test using $^{3}H_2O$, $^{32}PO_4$ and $^{15}NO_3$

3.4.1 Purpose of simultaneous injection

The main purpose of using different tracer substances simultaneously is that these provide information of fundamentally different transport processes that can be related to hydromechanical and biogeochemical mechanisms. Sampled data on the fate of tritiated water ($^{3}H_2O$ labeled water) provides information on hydromechanical mixing in the watercourse of water itself, including advection, in-stream dispersion and uptake in transient storage zones such stagnant surface water zones and the hyporheic zone. Transport of phosphate and nitrate is also governed by these hydromechanical mixing mechanisms, but is furthermore affected by reactions occurring in the flowing, open water column as well as in the transient and lateral storage zones. By first facilitating an independent evaluation of the hydromechanical mechanisms using tritiated water, the evaluation of the ^{32}P- and ^{15}N-labelled isotopes can be directed towards the biogeochemical reactions such as sorption and degradation.

3.4.2 Radiological risk assessment of tracer test

Tracer testing in a stream needs to undergo a thorough radiological safety assessment beforehand in order to assess the injected activity and duration of injection. The risk assessment should comprise the maximum possible dose (in Sieverts) to individual humans and has to account for the following pathways or aspects

- doses at the site of injection
- direct radiation from the water course
- oral intake from the stream water or indirectly from irrigated crops

In addition there are specific accidents like spillage or various related accidental releases to the environment that may have to be considered and subjected to risk minimization. This safety analysis also included ecosystem effects, all though this should not be the general design criterion for the tracer injection.

Table 3. Isotope characteristics and dose transfer coefficients according to SSI (2000)

	Energy, e, per emission, n	Dose coefficient for oral ingestion (Sv/Bq)	Dose coefficient for inhalation (Sv/Bq)	Proportion of ingestion in organs (-)
^{32}P	1.71 MeV	$2.4\ 10^{-9}$	$3.2\ 10^{-9}$	0.8
^{3}H in water	18.61 KeV	$1.8\ 10^{-11}$	$1.8\ 10^{-11}$	1.0

The ^{32}P labeled phosphoric acid is 91 times more energetic than ^{3}H-labeled water. The energy associated with each isotope can be obtained by multiplying the prepared activities (Table 5) with the energy associated with each energy emission (Table 3). The actual dose transfer to individual humans further depends on the decay of the energy in various media as well as the exposure space.

The direct radiological dose is given by D = A E, where D = dose (J/s), A = activity (Bq) = emissions per time (i.e. n/t), E = $1.602\ 10^{-19}$ e (J), e = energy per emission in electron volt (eV). Since, the radiological dose is commonly assed per weight of a human it is standard to normalize with a body weight of 80 kg, i.e. 1 Sievert (Sv) = 1 Joule/kg. Hence, the dose per weight and time, d (J/(kg h) = Sv/h) with account taken to all radiation can be expressed as

$$d = 3600\frac{D}{80} = 45AE = 7.209\,10^{-18}A\,e \quad (Sv/h) \qquad (1)$$

By using the activity of the most energetic isotope (^{32}P), 153 GBq, we get an hourly dose of 1,886 mSv/h, which is 125 times the annual dose (Table 4), or the annual dose is exceeded in one and half a minute.

Table 4 Maximum allowed radiological dose according to the regulations of the Swedish Radiation Safety Authority (SSMFS, 2008:51).

	Effective internal dose (oral ingestion) (mSv/year)	Equivalent dose to the lens of the eye (mSv/year)	Equivalent dose to skin (average dose over 1 cm^2) (mSv/year)
Employee	50	150	500
Members of the public	1	15	50

This means that several protective measures had to be undertaken at the site of injection:

- Protective shield in 10 mm Plexiglas behind which ampules can be opened with pincers.
- Injection container made with 10 mm Plexiglas on the inside and 10 mm steel outer shell.

The Plexiglas shield retards the emitted beta particles with same efficiency since the travel distance is less than 1 cm. The steel shield protects against possible bremsstrahlung generated in the Plexiglas material. Further, it is essential to keep the distance to ampules and containers with ^{32}P since its beta particles travel 60 m in air and this can be done by e.g. the use of pincers to hold ampules and protective gloves. It is especially important to protect the eyes by wearing glasses, which have three times lower dose limit than the body as a whole (Table 4).

Direct radiation from the watercourse should not be an essential factor for the design of the tracer experiment. However, the activity in the stream is indirectly important both for certain scenarios of oral intake as well as ecological effects. To reduce the maximum activity it is recommended to use a peristaltic pump with a plastic tube leasing the radioactive solute from the injection container directly to the stream water without contaminating the pump parts.

Furthermore, an essential risk scenario is oral intake either from the stream water or from agricultural products irrigated with stream water. Table 3 gives a direct translation of the activity obtained through oral intake to dose. Because of the significant dilution of the tracers in the stream water during a several hours prolonged injection one can show under certain assumptions of stream discharge and rates of injection that the maximum allowed annual dose requires drinking of several liters of stream water.

3.4.3 Performance of tracer injection

Both type of injection and the sampling procedure are of great importance for a successful tracer test. Wagner and Harvey (1997) showed that a continuous injection that result in breakthrough curves with a rising limb, a plateau and a falling limb, provides better information to evaluate parameters with low uncertainty than compared to slug injections, especially for cases with a high distribution of different transport times.
The simultaneous reactive tracer test was performed between the 2nd and 6th of December 2015 over a 6.2 km long stretch of the Tullstorps Brook. A simultaneous, constant rate injection of tritiated water together with ^{32}P- and ^{15}N-labelled isotopes was made just downstream of the dams connected to Jordberga Sockerbruk the 2nd December 2015 (Figure 5). Solutes were mixed with 20 l of stream water, before pumped continuously from an injection container into the stream. The injection container was designed specifically for inclusion and injection of radioactive samples, with regard to the safety aspects stated above. Researchers working with the injection procedure used protection clothes, gloves and glasses at all times. In addition personal radiation dosimeters were used to monitor the dose on all researchers. The stream water used to dilute the tracer solutes before adding them into the stream was prepared in advance in a 20 l plastic tank with a tap. 200 g labeled potassium nitrate (98% N^{15}-KNO_3) was diluted with some of the stream water and poured into the container before the radioactive tracers were added. The labeled phosphate ($^{32}PO_4$) and tritium ($^{3}H_2O$) was transported to the site in glass ampules surrounded by covers made of plastic and lead. The covers were removed behind a Plexiglas shield, moved with a gripping tool and placed in a lead crush tower attached to the injection container (Figure 6 top picture). A wedge was then mechanically pushed into the tower, which broke the glass ampules and released the liquid content to fall into the injection container. Both ampules were broken by the same procedure but it was done in two separate crush towers to enhance the reliability of the crushing procedure. The remaining stream water in the 20 l tank was then poured though the crossing towers, rinsing all of the remaining solutes into the injection container. A peristaltic pump (Figure 6 bottom left picture) was used to pump the solutes from the injection container into the stream at a rate of 0.11 l/min. The pumping continued for 3 hours between 13.30 and 16.30. During the pumping a 4 ml aliquot was taken from the injection container and diluted to 1:62500, in two steps, before sent to the laboratory. The injected activities and amounts are summarized in Table 5. Based on aliquots taken from the injection tank with 20 l injection solute, the activities of ^{3}H and ^{32}P were found to be 9.58 MBq/ml and 7.61 MBq/ml, respectively, which give total activities of 191.8 ± 2.3 GBq and 152.1 ± 1.8 GBq. One aliquot of 4 ml was taken and diluted 250 times before transportation to the laboratory where two aliquots where produced with a dilution of totally 62,500 times.

Table 5 Injected activity and amount.

Tritiated Water, H_3 (GBq)	192
Phosphoric (V) acid, H_3PO_4 (GBq)	152
Potassium nitrate, 98% N^{15}-KNO_3 (g)	200

Figure 6 Upper photo: Ampule with radioactive ^{32}P is moved from shielded transport container using pincer into "crush tower" of the injection container. The crush tower brakes the ampule so that the liquid falls down in the injection container from where it is pumped into the stream. Lower-left: Adjustment of pump to obtain appropriate injection time and stream activity at the site of injection. Lower-right: In-stream sampling procedure.

3.4.4 Investigated reaches and sampling procedure

Four different reaches were investigated trough the simultaneous tracer test and also in this case the sampling was planned to isolate the evaluation of processes occurring on reaches of specific character. In the first two of these reaches (S1-2 and S2-4), substantial remediation actions was performed 2009 and these are therefore referred to as "established remediation actions". Those two reaches are the same as the established, remediated reaches investigated with RWT (R1-2 and R2-3), only S2-4 covers a longer stretch of the stream than R2-3, since the downstream sampling was done at point 4 instead of point 3 (Figure 5). The discharge was considerably higher during the simultaneous tracer test compared to the conditions during the RWT tracer tests, leading to water-filling of flood zones that have been installed in a few places and flooding of the upper levels of the 2-step ditches, which was not the case in the RWT tracer tests. As a consequence of time passed since the installation of remediation actions, the two established

Figure 7. Visual comparison between reaches with established (left) and non-established remediation actions (right).

Table 6 Characteristics of the reaches investigated with the simultaneous reactive tracer test.

		Reach characteristics		
Reach No.	Reach type	X (m)	d (m)	w (m)
S1-2	**Established remediation actions (Sediment trap):** A deepening and widening of the stream channel aiming to slow down the water and allowing particles to sediment. Densely vegetated.	77	1	8
S2-4	**Established remediation actions (Figure 1a):** A variety of measures including engineered meandering, constructed riffle and pools, 2-step ditches, overflow wetlands and flooding zones. Objects such as boulders and logs evenly placed out along the stream bottom. Densely vegetated.	2350	0.42	3.75
S4-5	**Non-established remediated:** A variety of measures including engineered meandering, constructed riffle and pools, 2-step ditches, one flooding zone and one sediment trap. Objects such as boulders and logs evenly placed out along the stream bottom. No vegetation.	1740	0.37	3.33
S5-7	**Non-established remediated:** A variety of measures including engineered meandering, constructed riffle and pools, 2-step ditches and two sediment traps. Objects such as boulders and logs evenly placed out along the stream bottom. No vegetation.	2200	0.37	3.75

reaches had substantial vegetation in the stream channel. In contrast, the last two reaches in the simultaneous tracer test (S3-5 and S5-7), had just recently been modified. The recent installation of remediation actions led to stream channels without vegetation, which will be referred to as "non-established remediation actions" (Figure 7).

The reach characteristics are summarized in Table 6 and measuring sections for breakthrough curves are marked at the map in Figure 5. However, the average depth and width defines only the main channel and does not include any stagnant or low velocity surface water zones alongside the channel. No depth and width measurements were made in the sediment trap due to high water levels and therefore the parameters in row 1, Table 6, are only roughly estimated for this reach.

Samples were taken manually in the middle of the stream (Figure 5, bottom right picture), initially every half hour and later more rarely. A strategy was to take sufficiently dense samples during the rising and falling limbs of the breakthrough curves (Harvey and Wagner, 1997). The sampling continued during four days, to capture the slope of the breakthrough tail (eg. the part of the tracer with the longest residence times in the stream), which has shown to provide essential information regarding transient storage zones and the processes therein (Haggerty, 2002). Phosphate/tritium samples were taken in 50 ml plastic bottles and nitrogen samples were taken in 10 ml plastic sampling tubes containing 1 ml of sulfuric acid (1 moles/l) to prevent further biological activity. Some of the samples were filtered, using 0.45 µm filters, to gain information about the ratio of adsorbed versus non-adsorbed solute concentrations. The nitrate samples were kept outside for around 12 hours before they were placed in the freezer while the phosphorous/tritium samples were directly transferred into containers suitable for the analysis described in section 2.4.5. Outside air temperatures varied between 2 and 10 °C during the period of the sampling, according to the SMHI measuring station in Sturup, 13.6 km from the injection point. Samples at site 7 were taken with an automatic sampler and were therefore moved from its larger containers to the 10 ml plastic sampling tubes before frozen. The automatic sampler took samples of 100 ml and therefore 10 ml of acid were placed in the containers before samples were taken.

3.4.5 Beta counting analyses of $^{3}H_2O$, $^{32}PO_4$

Since ^{32}P and ^{3}H are pure beta emitters, liquid scintillation counting method is the best method to estimate the activity in water samples. Hence, the activity concentrations of tritium and ^{32}P in stream water samples were measured by liquid scintillation counting method with Quantulus 1220 liquid scintilator beta/alpha spectrometer at AGH UST laboratory. We used Quantulus 1220 and plastic 22 ml vials. The proportion of sample and scintillation for ^{32}P was 10ml sample and 10 ml of Insta-Gel Plus, for tritium we used 8 ml of sample and 12 ml of Ultima Gold scintillator. The ratio of scintillation and sample volumes was selected to get the best efficiency of the detection. For instance, increasing the scintillation liquid increases the probability for short travel distances for beta-emitted electrons to reach the scintillator compound. The same procedure was applied for the samples taken both in the stream water and the aliquots taken from the injection container (se section 2.4.3).

The left-hand side graph of Figure 8 shows the energy spectrum of internal standards used during the procedure to obtain the counting efficiency for both ^{3}H and ^{32}P. As we can see it is possible to measure both isotopes 32P and ^{3}H at the same time with only a small overlapping of energy windows for each isotope. Since about 3% of total counts of ^{32P} is present in the energy window of ^{3}H and the ratio 32P:3H in samples differs the simultaneous measurement of both isotopes overestimates tritium activity. To avoid that we have measured ^{3}H samples 4 months after experiment. Since, the half-life time of ^{32}P is 14,262 days, after 4 months the activity of ^{32}P decreases about 350 times. The half-life time of ^{3}H is 12,32 y so storage had decreased the activity by 2% of initial value at the time of measurements. The right-hand side graph of Figure 8 shows the energy spectrum of 3 samples from a site located 4012m downstream the injection point measured 2 weeks after the experiment. It can be seen that the activities of two first samples are at the background level and the 3rd sample whose specific activity during injection to the stream was (19,4+/-1,1) mBq/ml has built up a distinct spectrum. The details behind the relationship of counting and estimated activity are described in Appendix 1.

The measurements of ^{32}P were done immediately after the experiment due to the short half-time decay of ^{32}P (14 days). Activities of ^{32}P in samples were measured by counting in the energy window of 20keV-2000 keV in series of 20 samples in parallel with the standard (of activity 9,07+/-0,91 Bq/ml on 10.12.2016) and background sample. Scintillator was added to samples one day before measurement, than samples were kept in spectrometer to equilibrate thermally for 24h before the measurement. Neither samples of ^{32}P nor ^{3}H were filtered to decrease the risk of contamination and since PO_4^{3-} is easily sorbed. We estimated the average adsorption rate to be in the range of 6 - 76% between samples. Adsorption was prevented by by adding 0,1 ml of 0,1 N of H_3PO_4 before sampling in the field. The background sample for ^{32}P was an aliquot of a 1 l

sample of river water taken from Tullstorps Brook 1h before the injection of a tracer. At each series of measurments a new background sample was prepared with new scintillator.

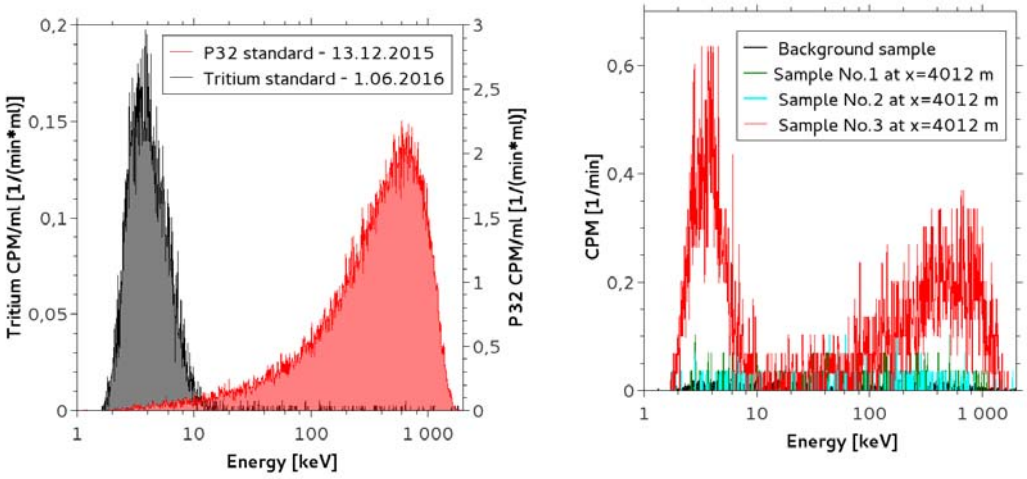

Figure 8 Left-hand side: Energy spectrum of 32P and tritum standards used in analyses. Right-hand side: Comparison of energy spectrum 3 samples and background sample at site located 4012m downstream the injection point.

The counting time varied from 30-360 minutes per sample and was adjusted to obtain the best precision and at the same time to minimize the effects of the rapid radioactive decay of this isotope. Measurements of tritium started 4 months after experiment in order to minimize the signal from ^{32}P in the samples. An internal standard was used. Each sample was measured for 30 minutes and repeated from 5-12 times. The number of runs was adjusted to the activity to get the best accuracy in reasonable time. The activities of samples were recalculated for the time of injection of tracers to the stream in order to compare the activities of phosphorus and tritium recovered during the experiment with the injected amounts. The background activities of ^{32}P and ^{3}H were evaluated by measuring activities of these isotopes in a "zero" sample collected from the stream before the injection of tracers. These background activities were determined separately for each batch of samples measured together in the LS counter as the detection conditions may vary between runs.

Activity of tritium (^{3}H) in samples were measured in parallel with the standard (of activity 1,01+/-0,10 Bq/ml on 13.04.2016) and background samples taken from river and dead water(tritium free). The additional sample of dead water was used to obtain the absolute activity of tritium in samples. Each sample was measured for 30 minutes and repeated from 5 to 12 times. The number of runs was adjusted to the activity to get the best accuracy in reasonable time. Samples ware measured in series to average effect of background variability of coming from the apparatus and cosmic radiation. The energy window for counting was set on region 0-18,6 keV.

3.4.6 Analyses of $^{15}NO_3$ (IM)

Nitrogen exists in two stable isotopes with atomic masses of 14 and 15. The lighter one, 14N, makes up 99.6337 % of the total nitrogen on earth and the remaining 0.3663 % is due to the heavier 15N. Because more energy is needed to break or form chemical bounds involving 15N than 14N, the lighter isotope generally reacts faster than the heavier (Robinson, 2001). Therefore, when part of a substrate is consumed or transformed in a bio- or physio-chemical process, the isotopic ratio $R = n_{15}/n_{14}$ $(-)$ (where n is number of atoms) will differ between the substrate and its product, a phenomena which is called fractioning (Bedard-Haughn et al., 2003). Out of convenience natural isotope ratios R_{sample} (-) is often expressed in comparison with a standard ratio $R_{standard}$ (-)according to:

$$\delta^{15}N = 1000 \left(\frac{R_{sample} - R_{standard}}{R_{standard}}\right) \qquad (2)$$

where $\delta^{15}N$ in Eqn. (2) is expressed in units of ‰ and the standard is the isotope ratio of the atmosphere. The isotope ratios can also be used to calculate the percentage of ^{15}N atoms in a sample A% according to:

$$A\% = 100\left(\frac{n_{15}}{n_{15}+n_{14}}\right) = 100\left(\frac{R_{sample}}{R_{sample}+1}\right) \quad (3)$$

Since the injection of total nitrate was rather small compared to the large amount of nitrate initially existing in the stream the total nitrate concentration in the stream will not be altered. However, it will still be possible to see a breakthrough of the $\delta^{15}N$ atomic percentage ^{15}N, although the signal might be damped by the large discharge of water and nitrate from the upstream main channel and possible infiltration from the surrounding soils. When using enriched nitrate as a tracer a mixing model has to be used to interpret the results. In order to separate the signal from the existing nitrate in the stream, the background isotope ratio and the tracer isotope ratio has to be considerably different and the fractioning between measuring points has to be negligible (Robinson, 2001). The total concentration of nitrate derived from the injected tracer, $c_{tracer}(\mu g/ml)$ can be calculated according to:

$$c_{tracer} = \frac{A\%(^{15}N_{sample}) - A\%(^{15}N_{background})}{A\%(^{15}N_{tracer}) - A\%(^{15}N_{background})} c_{N,total} \quad (4)$$

where $A\%(^{15}N_{sample})$ is the atomic percentage of ^{15}N in the sample, $A\%(^{15}N_{tracer})$ is the atomic percentage of ^{15}N in injected tracer and $A\%(^{15}N_{background})$ is the atomic percentage of ^{15}N in stream prior to the injection. $c_{N,total}(\mu g/ml)$ is the measured total nitrogen concentration in the sample.

The $^{15}NO_3$-samples from Tullstorps brook were kept frozen when transported to the joint laboratory at the Department of Forest Ecology and Management, at the Swedish University of Agricultural Sciences. Analyses were done using elemental analyzer isotope-ratio mass spectrometry (EA-IRMS), which is a technique for measurements of nitrogen and carbon isotope-ratios where the materials are being combusted or thermally converted in an oxygen atmosphere followed by a gas chromatography separating the evolved gases (Carter and Barwick, 2011). As a pre-treatment 750 µl of liquid samples were added to tin capsules and water was removed through evaporation in 70 °C, overnight. Thereafter the TIN capsules were introduced to the IRMS as solid samples. After the nitrate isotopes have been separated, as a last step in the IRMS, their quantities are analyzed using mass spectrometry. The numbers of ^{15}N and ^{14}N atoms are found in each sample through evaluation of the mass spectrums and results are reported as δN^{15} or atom percentage ^{15}N. In surface waters δN^{15} has an average value of around 10 ‰ (Bedard-Haughn et al., 2003), which can be expected as the background concentration in this investigation. The IRMS can identify δN^{15} values as low as 2 ‰ with an uncertainty of 0.3 ‰. Also the total nitrate concentration in the samples was evaluated from the mass spectrum and the tracer concentration in each sample was calculated using equation (4).

3.5 Evaluation of breakthrough curves

The overall objective with the addition of artificial tracers in streams is to characterize the solute transport along a specific stretch of the stream. The general approach consists of sampling the solute concentration at specific locations downstream of the injection point over time. By analyzing the distribution of concentration over time, the so-called breakthrough curves (BTCs), the solute response can be investigated. The response depends both on hydromorphological properties along the reach as well as solute specific characteristics. Often a conservative tracer such as ^{3}H is used to characterize the hydrological response of a reach, i.e. the hydromechanical transport and mixing processes in the stream environment. Due to the advection dominated transport, the bulk of the conservative tracer is shifted towards later arrival times for longer transport distances, which is clearly evident in the observed Rhodamine WT BTC from the tracer test in Tullstorps Brook 8th June 2015 (Figure 8). In addition, in-stream mixing processes such as hydrodynamic dispersion and exchange with surface and subsurface transient storage zones further alter the concentration distribution during the advective transport. As a result the peak values of the BTC's are decreasing and both the spreading and the asymmetry around the mean value are increasing as the tracer is transported downstream (Figure 8).

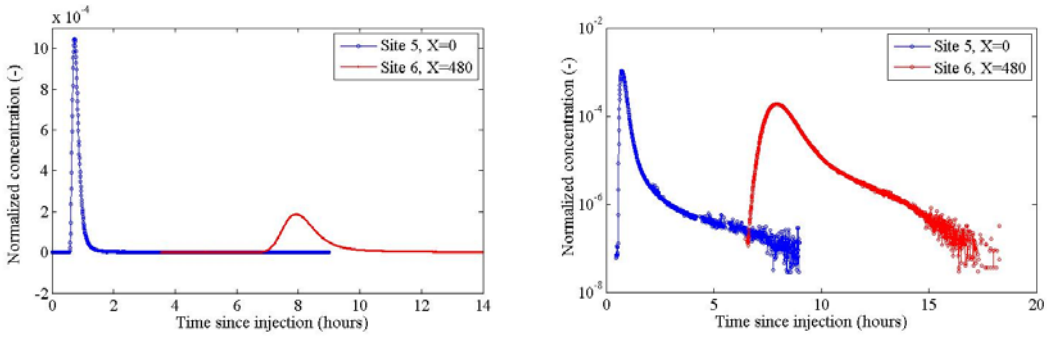

Figure 8. Rhodamine WT stream water concentration displayed with linear (left panel) and logarithmic concentration-axis (right panel) at the sampling stations in Tullstorps Brook.

By contrasting the behavior of a reactive and a conservative tracer the effect of biogeochemical reactions on the response of a reactive solute can be investigated. The implication of the additional effects of biogeochemical reactions on the BTC depends on the hydrologic conditions but also on reach specific characteristics, such geometry of the streambed, sediment properties (geological and biogeochemical) and density of in-stream vegetation, as well as the chemical affinity of the reactive solute. The effect of biogeochemical reactions can be interpreted by comparing of the observed BTCs of ^{3}H and ^{32}P from the simultaneous tracer experiment. This comparison revealed that in addition to the hydrodynamic retention ^{32}P was further retained in the stream (Figure 9). The effects of this biogeochemical retention are most apparent in the BTC's of ^{32}P as decreased peak concentration and an increased concentration at late times (more pronounced tailing) (Riml et al., 2013) that are consequence of the high affinity of phosphorous to sorb to streambed sediments, suspended solids and biofilms (Wörman et al., 2004; Whiters and Jarvie, 2008).

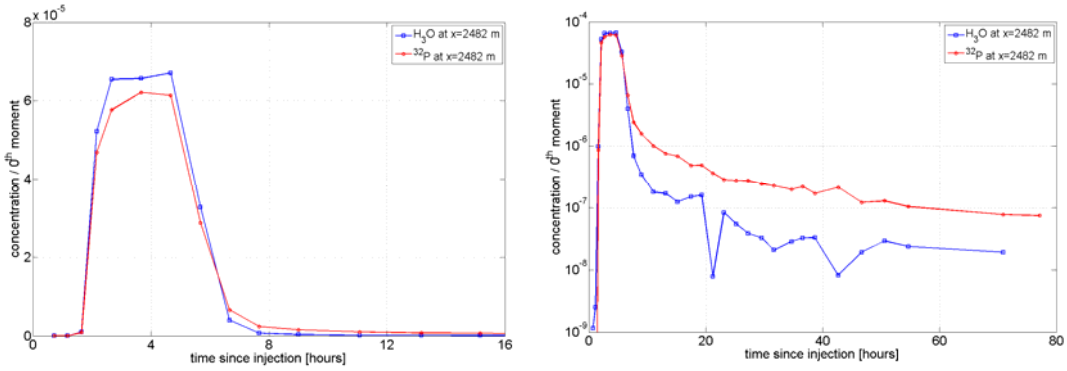

Figure 9. Comparison of ^{3}H (blue line) and ^{32}P (red line) concentrations sampling station S4. To illustrate the effect of sorption on both the peak and the tail of the BTC's the concentration is displayed using both a linear (left panel) and a logarithmic concentration axis (right panel). Note that the observed concentrations are normalized with their total observed mass at site S1 to enhance the comparison between the two substances.

3.5.1 Evaluation using temporal moments

The characteristics of a stream reach can be evaluated directly by calculating the temporal moments of the observed BTC (e.g. Schmid 2003, Wörman and Wachniev, 2007, Riml and Wörman 2011). Temporal moments are statistical descriptors of a sample distribution, which in this specific context relates to the distribution of transport times (i.e. the shape of the BTC) at a given distance downstream of the injection point. By comparing the relative change in temporal moments of observed BTCs at different locations in the stream, qualitative information regarding key transport processes along the reaches in-between stations can be investigated. The temporal moment, m, around the origin are defined according to:

$$m_k = \int_0^\infty t^k C(t) dt \qquad (5)$$

where m_k denotes the temporal moment k $[s^k]$, C is the concentration at a given distance from the injection $[kg/m^3]$. Important temporal moments for evaluating stream tracer tests are the zeroth and first temporal moments that provide measures of the mass recovery (relating to degradation of solute mass), and the expected transport time (relating to the retardation of solute mass), respectively. By normalizing the observed concentrations with the total injected mass according to:

$$c(x,t) = \frac{C(x,t)}{\int_0^\infty C(x,\tau) d\tau} \qquad (6)$$

, the zeroth temporal moment for a conservative tracer, m_0, becomes unity. The first temporal moment, m_1, is the expected value and can be used to define the central temporal moments, i.e. the moments around the expected value according to:

$$n_k = \int_0^\infty (t - \mu_t)^k c(t) dt \qquad (7)$$

, where n_k denotes the k^{th} central temporal moment $[s^k]$ and μ_t [s] is the expected value. Thus equation (7) can be used to derive important statistical measures of the BTC such as the variance, $\sigma_t^2 = m_2 - m_1^2$, and the skewness $S_t = m_3 - 3m_1(m_2 - m_1^2) - m_1^3$, that can be linked to both differences among stream reaches but also between solutes with different chemical affinity, i.e. different tendencies to undergo biogeochemical reactions in specific stream environments.

3.5.2 Evaluation of a tracer test using a transport model

In addition to evaluation of the temporal moments, the observed solute response for a specific stream reach can be evaluated using mathematical models. There exist a large body of solute transport models, with a common objective to provide quantitative information regarding key transport processes. Normally the models are divided into parametric (e.g. Boano et al. 2015 and references therein) and non-parametric methods (e.g. Payn et al., 2008; Gooseff et al. 2011). Although suffering from difficulties in model description and constraint that might lead to problems of equifinality (e.g. Beven 2009), the parametric methods are by far the most common method allowing for direct estimation of the governing hydrodymamic and biogeochemical processes.
For modeling purpose, the solute transport in streams are often assumed to follow 1D advection-dispersion equation with an additional exchange with slow moving, transient storage zones (e.g. Boano et al., 2015). The transient storage zones can be located in the surface water as stagnant side pockets (e.g. Choi and Harvey 2000, Briggs et al. 2009) or in the hyporheic zone that is defined as the region beneath and alongside the stream where there is mixing of surface water and shallow groundwater (e.g. Boano et al. 2015 and references therein). Here, we have adopted the model representation of Wörman et al. (2002) and further developed by Riml et al. (2013), that takes both the physical and biogeochemical transport processes into account. If we assume that the significance of the biogeochemical processes in the main channel is small, the solute concentration in the main channel can be defined according to:

$$\frac{\partial C_{MC}(x,t)}{\partial t} + u\frac{\partial C_{MC}(x,t)}{\partial x} - D\frac{\partial^2 C_{MC}(x,t)}{\partial x^2} = \frac{P}{A}J_S \qquad (8)$$

, where C_{MC} is the solute concentration $[kg/m^3]$, u is the main stream flow velocity $[m/s]$, D is the hydrodynamic dispersion $[m^2/s]$, P $[m]$ is the wetted perimeter of the main channel, and A $[m^2]$ is the cross-section area of the stream,. J_S is the solute mass flux between the main channel and adjacent storage zones $[kg/(m \cdot s^2)]$, resulting in an increased retention of the solutes due to hydrodynamical retardation but also to an additional retention of the solute due to the possible biogeochemical reactions that occurs in the transient storage zones. The solute concentration in the storage zone can be defined according to:

$$\frac{\partial C_{SZ}\eta}{\partial t} + \frac{V_z}{(1+K_{SZ})}\frac{\partial C_{SZ}}{\partial z} = -\lambda_{SZ}C_{SZ} \qquad (9)$$

, where C_{SZ} is the solute concentration $[kg/m^3]$, η is the sediment porosity $[-]$, V_z is the lateral flow velocity $[m/s]$, K_{SZ} is the equilibrium partitioning constant between dissolved and sorbed phases of the tracer [–], and λ_{MC} is the first order reaction rate $[s^{-1}]$ resulting in irreversible solute loss. The exchange between the main channel and the storage zone results in a distribution of residence times within the storage zone $f(T)$ and by assuming that $W = V_z/2$, the volumetric flux into and out of the storage zone $[m/s]$, is constant the net solute mass flux between the main channel and the storage zone $[kg/(m^2 s)]$ can be obtained by integrating over all possible residence times according to:

$$J_S = \int_0^\infty f(T)W(\tau,T)|_{\tau=T}(C_{SZ} - C_{MC})dT \qquad (10)$$

Thus, the model accounts for a transient storage defined by a pdf of residence times that conceptually can be viewed of as either a single storage zone with a distribution of residence times or a distribution of storage zones with different residence times. In general, $f(T)$ can take on any shape (i.e. statistical distribution), which opens for a high degree of flexibility in the description of the exchange with the storage zones. In addition, the observed values at the first sampling station can be used as the boundary condition and by assuming that no mass is initially availible in the system, i.e. $C(x, t = 0) = 0$, the simulated concentration at a given reach can be obtained by convolution of the boundary condition and the response of the subsequent reaches. An expression of the solute retention, can be defined by deriving the first temporal moment, according to equation (7), of the tracer concentration defined by equation (8)-(10). To find the

exact solution to the concentration certain assumptions are needed such as an exponential residence time distribution and a slug injection boundary condition $c(x = 0, t) = M_0/Au$, where $M_0[kg]$ is the injected mass. The resulting expected arrival time of the tracer is $\tau = (X/U)(1 + F)\ [s]$, where:

$$F = \frac{P}{A}\langle W\rangle\langle T\rangle\frac{(1 + K_{HZ})}{(1 + \lambda_{HZ}(1 + K_{HZ})\langle T\rangle)^2} \qquad (11)$$

is a dimensionless retention factor. For conservative solutes (i.e. $K_{HZ} = \lambda_{HZ} = 0$) F in equation (11) reduces to a pure hydrodynamical retardation factor previously defined by Wörman et al. (2002), that reflects the size ratio between the storage zone, WT, and the stream, A/P.

The model can be fitted to an observed concentration breakthrough, either by eye or through a formal optimization from which the model parameters can be estimated. When using the fit-by-eye method it is essential to have a general understanding about how different parameters eaffect the shape of the BTC (Harvey and Wagner, 2000), where for example the discharge (Q = uA) mainly affects the top concentrations and the stream velocity the arrival time of the peak, while transient storage parameters affect the shape the so called tail created by late time arriving solutes. In a formal optimization an object function, often the mean squared difference between the observed and modelled data, is minimized by changing the parameters of the model. Depending on the purpose of the study different formulations of the object function is more or less suitable, where formulations that empasize the tail of the breakthrough curve is essential to provide accurate estimates of transient storage parameters (Wörman and Wachniev, 2007). One way to empasize the tail is to compare the logarithm values of the concentrations, which decrease the importance of large concentrations compared to a linear comparison. However, with this approach there is a risk that accuracy in the parameters describing transportation of the bulk is lost. Bottacin-Busolin et al. (1993) did solve this problem by formulating an object function according to:

$$\varepsilon = \min_{\varepsilon}\left(\sqrt{\frac{1}{N_A+N_B}\left(\frac{\sum_{i=1}^{N_A}\left(C_{mod,A}-C_{obs,A}\right)^2}{\left(\max(C_{obs,A})-\min(C_{obs,A})\right)^2}+\frac{\sum_{i=1}^{N_B}\left(\log(C_{mod,B})-\log(C_{obs,B})\right)^2}{\left(\max(C_{obs,B})-\min(C_{obs,B})\right)^2}\right)}\right) \qquad (12)$$

where C_{mod} is the modelled concentration, C_{obs} the observed concentration and N_i is the total number of observations in group i. The root mean square error is here expressed either through logarithmic or linear values, depending on the position of the data-point in the breakthrough curve. Concentrations higher than a certain limit are treated as linear values (index A), while concentrations lower the limit are treated as logarithmic values (index B) in order to not overestimate errors in the peak.

4 Results

4.1 Rhodamine WT results

The evaluation of the tracer test data was performed through a formal optimization of the concentration data towards equation (8)-(10), using the object function stated in equation (12), where the limit between group A and group B where set to 20 % of the peak concentration. It was assumed that all reactions, such as adsorption and degradation of RWT in the transient storage zones were small enough to be neglected ($K_{sz} = \lambda_{sz} = 0$). The residence time distribution in the hyporheic zone (f(t)) was assumed to be exponential, thus defined by the average residence time $\langle T \rangle$ only. A visualization of the result is shown in Figure 10.

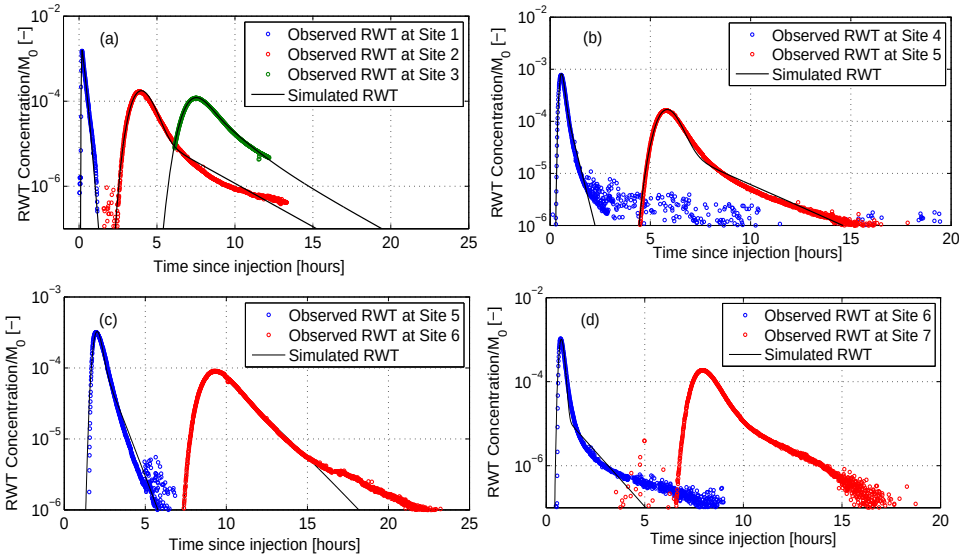

Figure 10. Observed and modelled normalized BTC from RWT tracer tests in Tullstorps Brook in; (a) 27/08 – 2014, (b) 10/06 – 2014, (c) 08/06-2015 and (d) 29/08 – 2015. The four tracer tests were performed in five different reaches (R1-2, R2-3, R4-5, R5-6, R6-7).

The optimization of the RWT breakthrough curves resulted in parameters that varied considerably between reaches (Table 7). The two remediated reaches, the sediment trap (R1-2) and the reach with a variety of different implemented remediation actions (R2-3) did have lower in stream velocities compared to the other reaches, which was expected due to the larger cross sections, more meandering and the large amounts of hindering objects, such as logs and boulder, present in the stream. Further, although dispersion coefficients in the two remediated reaches are relatively low, the Pe-numbers, $Pe = XU/E$, indicate that the relative importance of dispersion compared to advection is larger in the restored reaches compared to the unrestored. Also hyporheic exchange velocities, W, which varied between 7.63 10^{-6} m/s and 3.07 10^{-5} m/s, were largest in the sediment trap, followed by the other remediated reach. The total effect of the transient storage parameters on the retention factor F did not follow a clear trend connected to the remediation actions. The highest value (F = 0.33) is found in the more pristine reach (R5-6) and the lowest in the non-remediated reach R6-7 (F = 0.11).

Table 7 Parameters from optimization of RWT tracer test data

Reach	R1-2: Sediment trap	R2-3: Established remediated	R4-5: Non-remediated agricultural	R5-6: Non-remediated natural	R6-7: Non-remediated agricultural
Date of tracer test	27 Aug 2014	27 Aug 2014	10 Jun 2015	08 Jun 2015	29 Aug 2015
$u\ [m/s]$	0.006	0.009	0.081	0.019	0.055
E (m^2/s)	0.005	0.16	0.52	0.03	0.13
W (m/s)	$3.07\ 10^{-5}$	$2.29\ 10^{-5}$	$7.22\ 10^{-6}$	$7.63\ 10^{-6}$	$6.75\ 10^{-6}$
$\langle T \rangle$ (s)	$7.15\ 10^{3}$	$2.97\ 10^{3}$	$7.89\ 10^{3}$	$4.78\ 10^{3}$	$4.02\ 10^{3}$

4.2 Simultaneous test with $^{3}H_2O$, $^{32}PO_4$ and $^{15}NO_3$

The simultaneous tracer test with ^{3}H, ^{32}P, and ^{15}N performed in December 2016 was evaluated along 4 different reaches (Table 6) based on the observed breakthrough curves shown in Appendix 2. The analysis was performed for ^{3}H, ^{32}P and ^{15}N, but due to analytical problems caused by high uncertainties/low detection limits only a very limited analysis of ^{15}N could be performed. The observed BTC was used in a direct way to calculate the temporal moments (Eqn. 5-7), providing key statistical measures of the BTC that are connected to specific characteristics of the reaches. From estimations of mass recoveries (Fig. 11 top left panel), it is clear that a significant amount of the tracers observed at the first sampling station S1 was not recovered in the subsequent BTC's. The overall mass loss for the conservative tracer ^{3}H indicates that there was still significant tracer left in the system when the sampling was finished, which is also evident in the BTCs as the last curves did not reach the background concentration (Figure 9). This indicates the existence of storage zones with very long residence times that slowly releases tracer back to the main channel. Another explanation for a reduced mass recovery is a substantial dilution effect caused by lateral inflows of water that decreased the concentration of the tracer. Both these explanatory models are possible, especially during these high flow conditions preceded by large amounts of precipitation. However, there is no possibility in distinguishing between these two effects based on observed concentrations alone. Moreover, the additional mass loss of the reactive tracers ^{32}P and ^{15}N is small, indicating that the biological degradation or irreversible sorption of these substances was not profound during the experiment.

The first moment (expected transport time) increases more or less linearly with distance, which is as expected if the mean transport velocity is fairly constant in space. The first two central moments (the variance and skewness) on the other hand display a high degree of variability both for ^{3}H and ^{32}P along the four reaches. For the conservative tracer ^{3}H the analysis showed profound increasing values during the first (S1-2) and the third reaches (S4-5), a moderate increase during the second reach (S2-4) and a constant value during the last reach (S5-7). These findings are also evident in Figure 9, where the physical retardation is displayed as an increased tailing of the BTC. Moreover, the biogeochemical retardation increased the values of all moments of ^{32}P compared to ^{3}H. The prolonged holding times and additional tailing in the BTC due to sorption of ^{32}P was found to be especially large in the first (S1-2) and the second reach (S2-4), which are the reaches with established remediation actions.

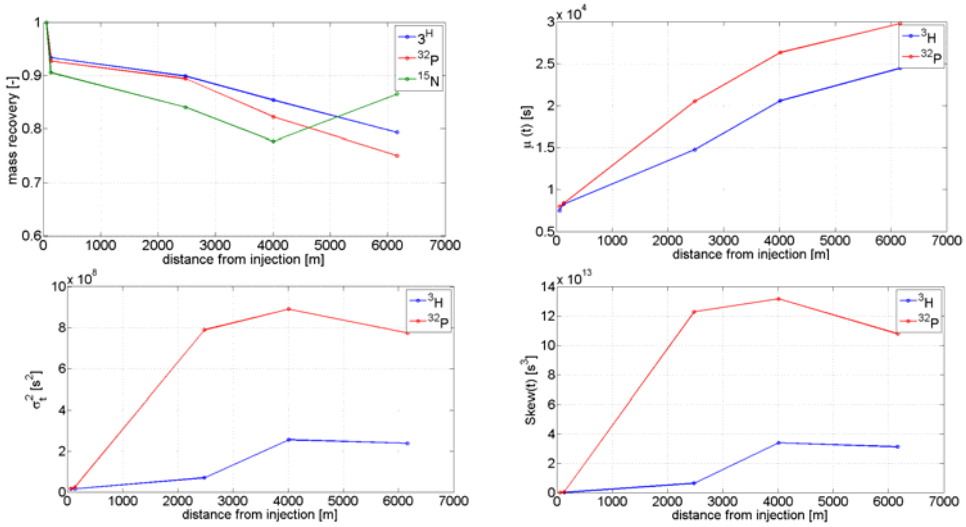

Figure 11. Statistical measures of the ^{3}H (blue), ^{32}P (red) and ^{15}N BTC (green) at different distances from the injection site including mass recovery (top left panel), mean value (top right panel), variance (bottom left panel), and skewness (bottom right panel).

In addition to the moment analysis, a more detailed analysis of the tracer test with possibilities to quantify the retention parameters was obtained by using the transport model (Eqn. 5-7). Due to the aforementioned methodological problems with ^{15}N, the model evaluation was done only for ^{3}H and ^{32}P. Here, a simultaneous fit-by-eye optimization of both conservative and reactive solutes was performed using a log-normal pdf of residence times in the storage zone to estimate the model parameters (Table 8). The primary focus of the simultaneous tracer experiment was to quantify the parameters describing the physical retention, i.e. W the volumetric flux of water between the main channel and transient storage zone and T the residence time within the storage zone, as well as the biogeochemical retention parameters, i.e. K_{SZ} the sorption of the storage zone and λ_{SZ} the first order decay in the storage zone that further affects the solute transport.

Table 8. Estimated model parameters from fit-by-eye optimization of simultaneous tracer experiment with ^{3}H and ^{32}P

Model paramter	Reach S1-2	Reach S2-4	Reach S4-5	Reach S5-7
$E\ [m^2/s]$	$1.0 \cdot 10^{1}$	$5.0 \cdot 10^{2}$	$5.0 \cdot 10^{1}$	$7.2 \cdot 10^{1}$
$u\ [m/s]$	$1.4 \cdot 10^{-1}$	$4.2 \cdot 10^{-1}$	$4.3 \cdot 10^{-1}$	$4.5 \cdot 10^{-1}$
$W\ [m/s]$	$2.0 \cdot 10^{-5}$	$1.5 \cdot 10^{-5}$	$2.0 \cdot 10^{-6}$	$1.0 \cdot 10^{-7}$
$T\ [s]$	$8.0 \cdot 10^{3}$	$5.5 \cdot 10^{3}$	$1.0 \cdot 10^{6}$	$4.0 \cdot 10^{5}$
$CV_T\ [-]$	$5.3 \cdot 10^{1}$	$1.3 \cdot 10^{2}$	$2.5 \cdot 10^{1}$	$3.2 \cdot 10^{1}$
$K_{SZ}\ [-]$	$3.5 \cdot 10^{1}$	$3.5 \cdot 10^{1}$	0	0
$\lambda_{SZ}\ [1/s]$	-	-	-	-

The model optimization provides a good fit between the observed and simulated concentration for both ^{3}H and ^{32}P (Figure 12-13). From the optimized values of ^{3}H (Table 8) a particular high value of the hydrodynamical retardation was found for the reach S4-5 ($F = 5.4$) that is more than one order of magnitude greater than the other reaches. For a sorbing solute like ^{32}P, an additional biogeochemical retardation that is proportional to $(1 + K_{SZ})$ will further affect F. The optimization revealed a strong biogeochemical retardation with K_{HZ}=35 for the first two reaches (S1-2 and S2-4) with established remediation actions, increasing the F factor to 5.6 and 3.0 respectively. On the contrary, in the last two reaches with non-established remediation actions (S4-5 and S5-7) K_{SZ} was found to be 0, resulting in no additional biogeochemical retardation.

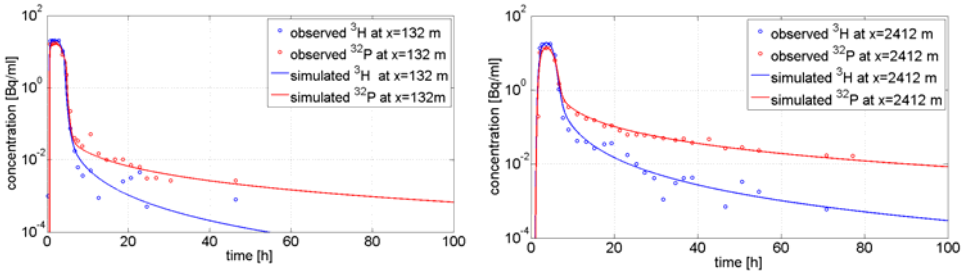

Figure 12. Comparision of observed and simulated concentrations of ^{3}H (blue) and ^{32}P (red) at S2 (left panel) and at S3 (right panel), i.e. for the reaches with established remediation actions. The simulated physical retention parameters are constans in each panel (E, u, W, T, CV_T) while an additional biogeochemical retention due to sorption ($K_{SZ} = 3.5 \cdot 10^1$) resulting in an increased tailing of the reactive ^{32}P compared to the conservative ^{3}H.

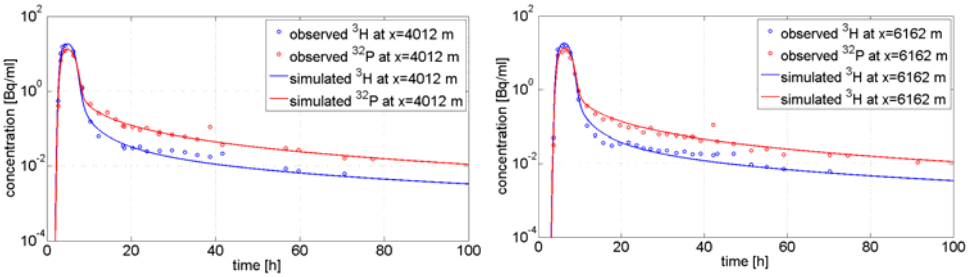

Figure 13. Comparision of observed and simulated concentrations of ^{3}H (blue) and ^{32}P (red) at S5 (left panel) and at S7 (right panel) i.e. the reaches with non-established remediation actions. The simulated physical retention parameters are constant in each panel (E, u, W, T, CV_T) whithout any additional biogeochemical retention due to sorption ($K_{SZ} = 0$) resulting in an proportional tailing of the reactive ^{32}P compared to the inert ^{3}H.

5 Discussion and conclusions

This report contains a thorough description of the key preparatory, experimental and evaluative steps when performing a stream tracer test. Although without the intention to cover all aspects, the report aims to describe a methodology that combines field experiments and mathematical transport model with the purpose to quantify nutrient retention and attenuation processes. Special emphasis of both the design of the tracer test and the subsequent evaluation lies on the connection between nutrient export, and the main drivers of solute transport in a stream: hydrological conditions as well as biological and geomorphological characteristics of the specific stream reach. The overall incentive to perform the tracer test in Tullstorp Brook was to investigate the effectiveness of implemented in-stream remediation actions with respect to hydromechancial and biogeochemical retention. Although increasing efforts are made worldwide to restore or remediate the ecological and chemical status of surface water systems (Nakamura et al., 2006, Bernhardt et al. 2005, Nienhuis and Leuven; 2001), quantitative evaluations of these measures targeting water quality parameters, such as nutrient concentrations, are generally lacking. In addition, the simultaneous stream tracer test using ^{3}H, ^{32}P, and ^{15}N is for the first time conducted in Tullstorps Brook and presented in this report.
The preliminary findings when comparing the individual tracer tests both using the four Rhodamine WT experiments and simultaneous ^{3}H, ^{32}P and ^{15}N experiment in the Tullstorps Brook include:

- Only insignificant change in the hydromechanial retention was found during the two different hydrological conditions that prevailed during the RWT and radioactive tracer tests. At least this was the case for the two reaches that did not undergo additional changes in geomorphology through remediation actions.
- A considerable increase in hydromechanical retention was found in one reach (S3-5), in which large remediation actions (such as flooding zones, sediment traps etc.) were implemented during the time period of the experiments.
- The importance of vegetation on the biogeochemical retention of ^{32}P was substantial, when comparing the established reach with dense vegetation and the not established reaches where vegetation in the stream and on connected flood areas had not yet grown up.

These findings indicate that the implemented remediation actions have a direct impact on the retention of nutrients from the Tullstorp Brook. In addition, seasonal variability and time since the construction (i.e. the degree of establishment) of the remediation actions are important to consider when evaluating the effectiveness of implemented measures.

6 Ackowledgements

The authors are sincerely greatful for review comments provided by Jens Christian Refsgaard, GEUS, Denmark, and René Chapell, SMHI, Sweden.

Appendix 1: Relationship between beta-counting and sample activity

The method of standard addition was not apllied because of large number of samples that had to be analysed for ^{32}P in a limited time. The correspondence between counting rates and sample activities was found by evaluation of detection efficiency. Matrix effect were not addressed, however, one can assume a large homogeneity of the collected water samples in conditions of high river stage and large water velocities.

Both tritium and ^{32}P activity ware calculated basing on efficiency of detection:

$$A_{measured} = \frac{\left(CPM_{sample} - CPM_{background}\right)}{eff}$$

$$eff = \frac{CPM_{standard} - CPM_{background}}{DPM_{standard}}$$

where : $A_{measured}$ = activity of sample at time of measurement, Eff = efficiency of detection, CPM_{sample} = counts per minute for measured sample, $CPM_{background}$ = counts per minute for background sample, $CPM_{standard}$ = counts per minute for standards and $DPM_{standard}$ = decay per minutes for standards (Activity of standard).The specific activities of all samples were recalculated on the time of injection basing on half time of decay, time lapsed between measurement and injection to the stream and volume of sample.

$$a_{experiment} = \frac{A_{measured}}{V} \circ e^{\frac{-\Delta t \circ ln(2)}{T_{\frac{1}{2}}}}$$

where $a_{experiment}$ = specific activity of sample [Bq/ml] at the time of injection of tracer to stream (13:00 2.12.2015), $A_{measured}$ = activity in sample at the time of measurement, V = volume of sample (8ml for H3, 10ml for P32), Δt = time between measurement and injection and $T_{1/2}$ = half–life time of isotope

Uncertainty of activities were calculated basing on uncertainty of counts and uncertainty of volume.

$$u\left(a_{experiment}\right) = a_{experiment} * \sqrt{\left(\frac{u(A_{measured})}{A_{measured}}\right)^2 + \left(\frac{u(V)}{V}\right)^2}$$

$$u(A_{measured}) = A_{measured} * \sqrt{\frac{u^2\left(CPM_{sample}\right) + u^2\left(CPM_{background}\right)}{\left(CMP_{sample} - CPM_{background}\right)^2} + \frac{u^2(CPM_{standard}) + u^2\left(CPM_{background}\right)}{\left(CMP_{standard} - CPM_{background}\right)^2}}$$

Appendix 2: Breakthrough curves observed from simultaneous tracer test

This appendix contains all observed breakthrough curves from the simultaneous tracer test performed in Tullstorps Brook 02/12/2015-06/16/2015. The original data can be seen on request to the authors of this report.

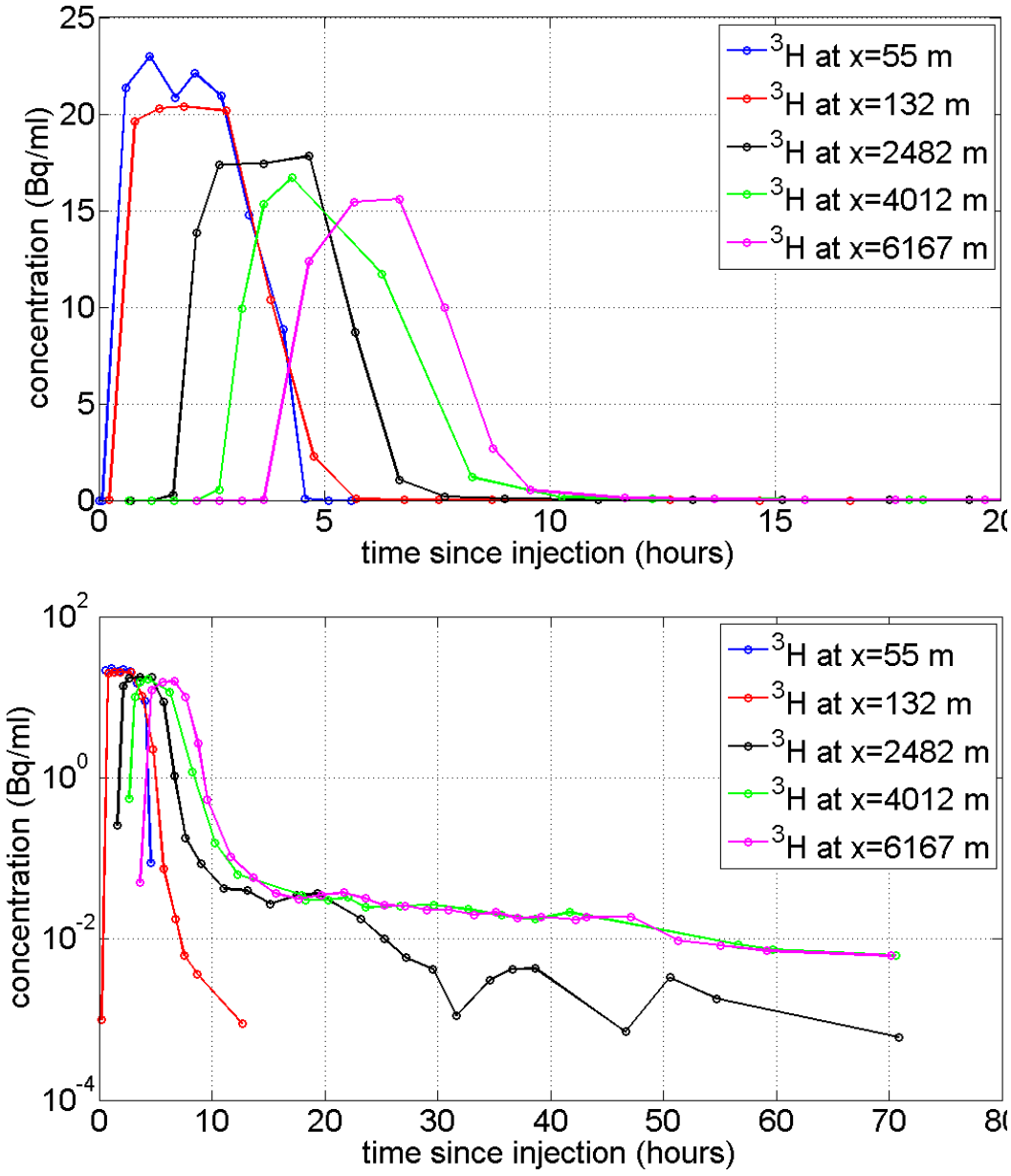

Figure A1. Observed stream water concentration of ^{3}H at 5 different sampling stations in Tullstorp Brook for the simultaneous tracer injection on the 2nd of December 2015. To emphasize different parts of the breakthrough curve the graph is shown here with linear (upper panel) and logarithmic concentration axis (lower panel).

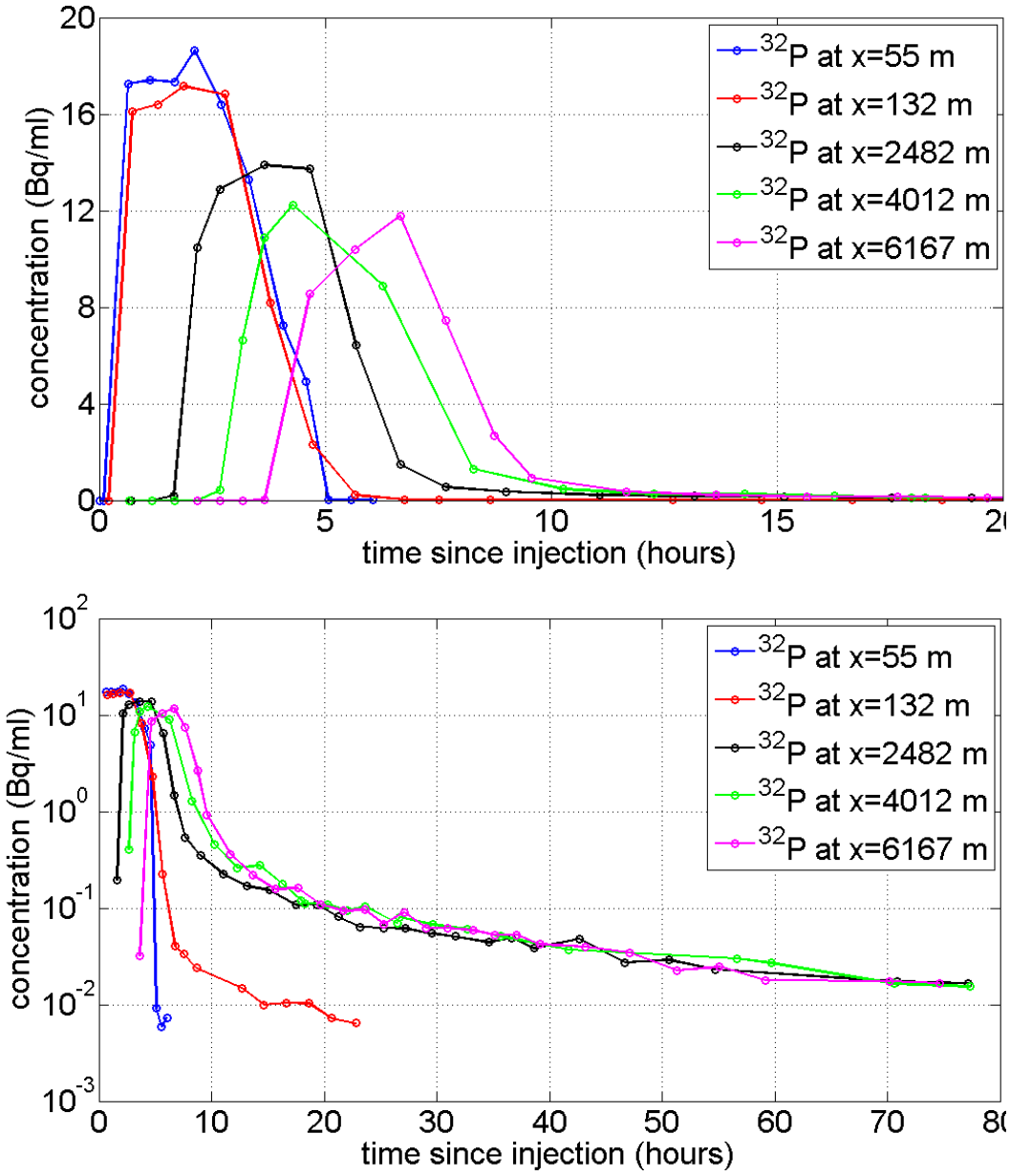

Figure A2. Observed stream water concentration of ^{32}P at 5 different sampling stations in Tullstorp Brook for the simultaneous tracer injection on the 2nd of December 2015. To emphasize different parts of the breakthrough curve the graph is shown here with linear (upper panel) and logarithmic concentration axis (lower panel).

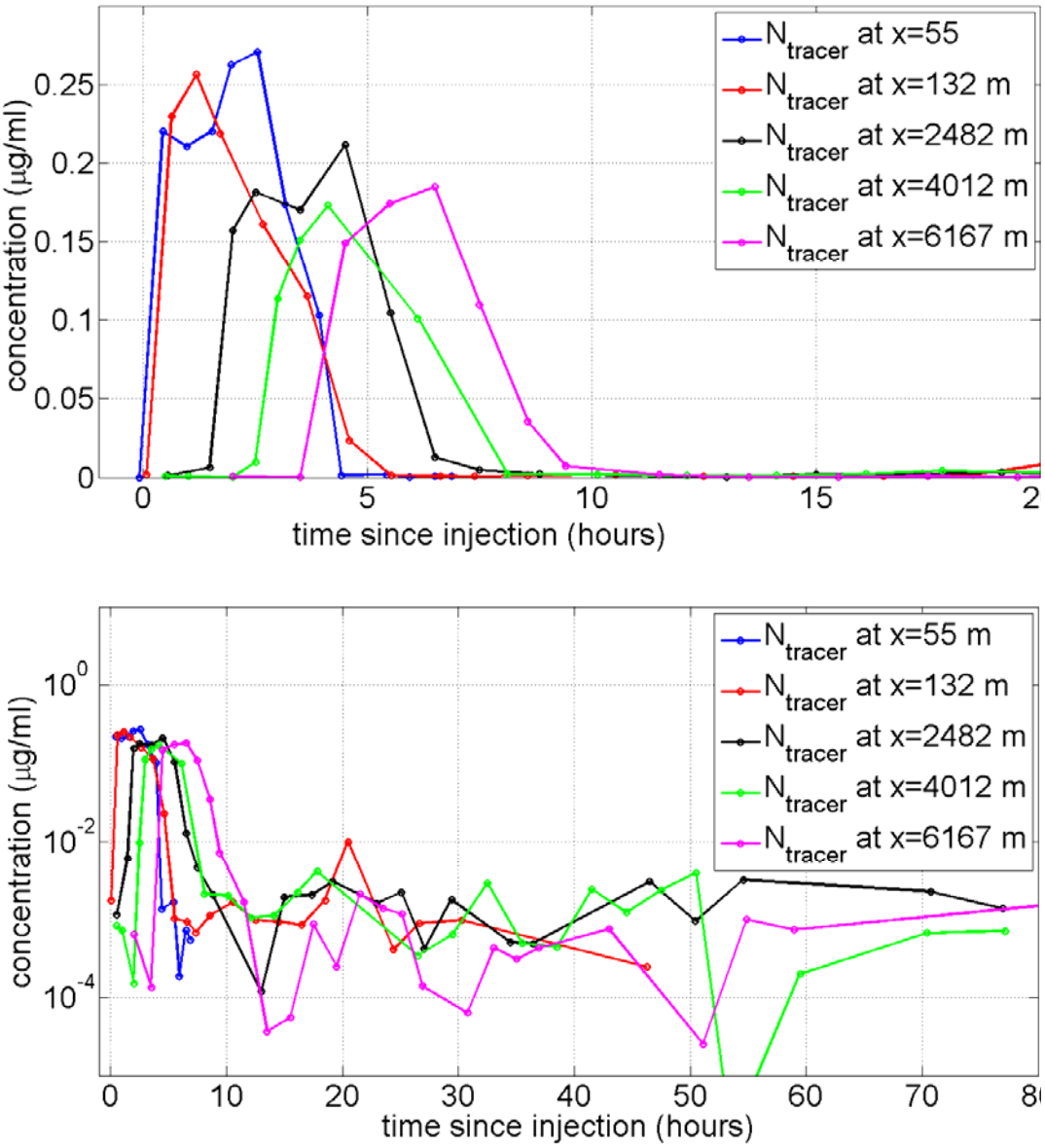

Figure A3. Observed stream water concentration of N deriving from the enriched tracer $^{15}NO_3$ at 5 different sampling stations in Tullstorp Brook for the simultaneous tracer injection on the 2nd of December 2015. To emphasize different parts of the breakthrough curve the graph is shown here with linear (upper panel) and logarithmic concentration axis (lower panel).

References

Arheimer, B., Löwgren, M., Pers, B.C. and Rosberg, J. 2005. Integrated catchment modeling for nutrient reduction: scenarios showing impacts, potential and cost of measures. Ambio 34(7):513-520.

Andersson, L. and Arheimer, B., 2003. Modelling of human and climatic impact on nitrogen load in a Swedish river 1885-1994. Hydrobiologia 497(1-3):63-77.

Bernhardt, E. S., M. A. Palmer, J. D. Allan, G. Alexander, K. Barnas, S. Brooks, et al. 2005. Synthesizing US river restoration efforts. Science 308:636–637.

Bedard-Haughn, A., J. W. van Groenigen, and C. van Kessel (2003), Tracing 15N through landscapes: potential uses and precautions, *Journal of Hydrology*, *272*(1–4), 175-190.

Beven, K. 2009. Environmental modelling: An uncertain future?, New York, USA, Routledge.

Boano, F., Harvey, J.W., Marion, A., Packman, A.I., Revelli, R., Ridolfi., L., Wörman, A., 2014. "Hyporheic flow and transport processes: Mechanisms, models, and biogeochemical implications", Reviews of Geophysics. Volume 52, Issue 4, pages 603–679, December 2014, doi: 10.1002/ 2012RG000417

Bottacin-Busolin A, Marion A, Musner T, Tregnaghi M, Zaramella M. Evidence of distinct contaminant transport patterns in rivers using tracer tests and a multiple domain retention model. Adv Water Resour 2011;34:737–46.

Briggs, M. A., Gooseff, M. N., Arp, C. D. & Baker, M. A. 2009. A method for estimating surface transient storage parameters for streams with concurrent hyporheic storage. Water Resources Research, 45.

Castro, N.M., Hornberger, G.H., 1991, "Surface-Subsurface Water Interactions in an Alluviated Mountain Stream Channel, Water Res. Res., 27(7), 1613-1621

Cardenas, B., 2015. Hyporheic zone hydrologic science: A historical account of its emergence and a prospectus, Water Resources Research 51(5): 3601-3616. 10.1002/2015WR017028

Carter, J.V., and V. J. Barwick (Eds), Good practice guide for isotope ratio mass spectrometry, FIRMS (2011). ISBN 978-0-948926-31-0

Choi, J., Harvey, J. W., Conklin, M. H. 2000. Characterizing multiple timescales of stream and storage zone interaction that affect solute fate and transport in streams. Water Resources Research, 36, 1511-1518.

Field M.S. et al (1995), An assessment of the potential adverse properties of fluorescent tracer dyes used for groundwater tracing, Environmental Monitoring and Assessment 38, 75-96, 1995

Fölster, J., Kyllmar, K., Wallin, M., Hellgren, S., 2012. Kväve- och fosfortrender i jordbruksvattendrag - Har åtgärdena gett effekt?, Institutionen för vatten och miljö, SLU Box 7050, 750 07 Uppsala Rapport 2012:1

Harvey, J. W., and B. J. Wagner (1997), Experimental design for estimating parameters of rate-limited mass transfer: Analysis of stream tracer studies,
Water Resour. Res., 33(7), 1731– 1741.

Harvey, J. W., and B. J. Wagner (2000), ‘‘Quantifying hydrologic interactions between streams and their subsurface hyporheic zones,’’ in Streams
and Groundwaters, J. B. Jones and P. J. Mulholland (eds.), Academic Press, San Diego.

Kilpatrick, F.A and J.F. Wilson, Jr. (1989), Measurement of time of travel in streams by dye tracing, Techniques of Water-Resources Investigations of the United States Geological Survey, USGS, Book 3, Applications of Hydrology.

Kunkel, U. and Radke, M. (2011), Reactive tracer test to evaluate the fate of pharmaceuticals in rivers, Environmental Science and Technology 45, 6296-6302

Nakamura, K, Tockner, K and Amano, K (2006) River and Wetland Restoration: Lessons from Japan BioScience 56 (5): 419-429

Nienhuis, P.H. and Leuven, R.S.E.W. (2001) River restoration and flood protection: controversy or synergism?
Hydrobiologiahttp://search.proquest.com/assets/r20161.9.1.366.866/core/spacer.gif444.1-3http://search.proquest.com/assets/r20161.9.1.366.866/core/spacer.gif, 85-99.Olofsson, H. (2015), Vattenundersökningar i TULLSTORPSÅN 2014/2015, Tullstorpsån Ekonomisk Förening.

Payn, R. A., Gooseff, M. N., Benson, D. A., Cirpka, O. A., Zarnetzke, J. P., Bowden, W. B., McNamara, J. P., Bradford, J. H. 2008. Comparison of instantaneous and constant-rate stream tracer

experiments through non-parametric analysis of residence time distributions. Water Resources Research, 44.
Riml, J., A. Wörman, U. Kunkel, and M. Radke (2013), Evaluating the fate of six common pharmaceuticals using a reactive transport model: Insights from a stream tracer test, *Sience of the Total Environment*, *458-460*, 344-354.
Rowinski, P.M. and Chrzanowski M.M. (2011), Influence of selected flourescent dyes on mall aquatic organisms, Actic Geophysica 59, 91-109
Runkel, R. L. (2015), On the use of rhodamine WT for the characterization of stream hydrodynamics and transient storage, *Water Resources Research*, *51*(8), 6125-6142, doi: 10.1002/2015WR017201.
Schmid, B. H. 2003. Temporal moments routing in streams and rivers with transient storage. Advances in Water Resources, 26, 1021-1027.
SSI, 2000. ”Doskoefficienter för beräkning av interna doser”, SSI Rapporter 2000:05: Avdelningen för personal och patientstrålskydd.
Svensson, 2014, A case study: The Tullstorp Stream Project - success factors, challenges and recommendations for improvement of agri-environmental projects, Baltic Compact, Swedish Board of Agriculture.Tullstorpsån Ekonomisk Förening (nd.), *Välkommen till Tullstorpsånprojektet!,* Tullstorpsånprojektet, http://www.tullstorpsan.se/index.php [2016-11-18].
VISS (2016), *Tullstorpsån (Skateholmsån),*VISS Vatteninformationssystem Sverige, http://viss.lansstyrelsen.se/Waters.aspx?waterEUID=SE614633-134828&timelineDateID=0 [2016-11-18].
Wilson, Jr, J.F., Cobb, E.D. and Kilpatrick, F.A. (1986) Fluorometric procedures for dye tracing, Techniques of Water-Resources Investigations of the United States Geological Survey, USGS, Book 3, Applications of Hydrology.
Withers, P.J.A. and Jarvie, H.P. (2008) Delivery and cycling of phosphorus in rivers: A review, Sci Total Environ. 400:379–395
Wörman, A., Packman, A.I., Jonsson, K., Johansson, H., 2002. "Effect of Flow-Induced Exchange in Hyporheic Zones on Longitudinal Transport of Solutes in Streams and Rivers", Water Resources Research: 38(1), 2:1-15.
Wörman, A., B. Kløve, and P. Wachniew (2004), Kinematic model of solute transport in stream networks: Example with phosphate retention in Morsa watershed, Norway, Arch. Hydro Eng. Environ. Mech. 51 (1), 41–53.
Wörman, A. and Wachniew, P., 2007. ”Reach scale and evaluation methods as limitations for transient storage properties in streams and rivers”, Water Resources Research, doi:10.1029/2006WR005808.

This page has intentionally been left blank

The present work has been carried out within the project ‘Reducing nutrient loadings from agricultural soils to the Baltic Sea via groundwater and streams (Soils2Sea)’, which has received funding from BONUS, the joint Baltic Sea research and development programme (Art 185), funded jointly from the European Union’s Seventh Programme for research, technological development and demonstration and from The Danish Council for Strategic Research, The Swedish Environmental Protection Agency (Naturvådsverket), The Polish National Centre for Research and Development, The German Ministry for Education and Research (Bundesministerium für Bildung und Forschung), and The Russian Foundation for Basic Researches (RFBR).